Collisional energy transfer modeling in non-equilibrium condensing flows

Natalia Gimelshein[*], Ingrid Wysong[†] and Sergey Gimelshein[*]

[*]*ERC, Inc, Edwards AFB, CA 93524*
[†]*Propulsion Directorate, Edwards AFB, CA 93524*

Abstract. Inelastic energy transfer rates between dimers and monomers have been found to be important in reproducing the equilibrium constant for dimers in a kinetic model. Molecular dynamics and DSMC models for energy transfer in argon dimer - argon monomer collisions are compared. The effective inelastic collision number for these collisions is evaluated, and found to decrease significantly when gas temperature increases.

Keywords: Homogeneous condensation, energy transfer, molecular dynamics, DSMC
PACS: 51.10.+y

INTRODUCTION

Theoretical, experimental, and computational studies of homogeneous condensation have drawn much attention over the last decades, mainly because this phenomenon plays an important role in many atmospheric and technological processes, and understanding its physical mechanisms and dependencies is critical for a number of engineering applications. One of such applications, pertaining to rocket vehicle operations at very high altitudes, is related to thruster plume expansion into the surrounding rarefied atmosphere [1]. Condensation in rapidly expanding flows has been observed experimentally as early as the 1930s [2], and has been extensively studied in the following decades (see for example [3] and the references therein). Computational modeling of expanding condensing flows has a shorter, although still respectable, history. In the past, two different approaches have been used to describe homogeneous condensation and, in particular, cluster nucleation (formation of small clusters from monomers) in the non-equilibrium environment of rapid expansions. The first approach is based on the classical nucleation theory, and is in fact a macroscopic approach that uses equilibrium thermodynamics and the principle of detailed balance to calculate the cluster size evolution and properties.

The second approach is a kinetic, microscopic approach, often based on the direct simulation Monte Carlo (DSMC) method to describe the flow behavior. The DSMC method has been used to study the process of cluster formation and evolution for a number of years. Over the last decade, it has been extensively and successfully applied to modeling the processes of cluster formation and evolution in supersonic jets by Levin et al. (see, for example, [4, 5]). The model initially was based on the classical nucleation theory, with the new clusters being formed at the critical size. Further work of these authors [4] extended the kinetic dimer formation approach of Ref. [6], where it was assumed that a ternary collision always results in a dimer formation, to include molecular dynamic (MD) simulations for obtaining information on the probability of dimer formation in such ternary collisions.

More recently, the first-principles kinetic theory was used [7, 8] to construct a DSMC based model that uses a kinetic RRK algorithm [9] to characterize the cluster evaporation rates, and an energy dependent collision procedure similar to the recombination reaction model of Ref. [10] for the collision complex formation. An empirical parameter was introduced for the inelastic collision number in the cluster-monomer collisions, and the Larsen-Borgnakke (LB) principle [11] was extended to simulate the energy transfer in collisions among monomers and clusters. This principle was also used for the energy redistribution in the dimer formation process. The model [7] was then adapted and extended to a combined Lagrangian-Eulerian approach [12], that maintains the benefits of a kinetic treatment of the homogeneous nucleation process while having a significantly higher computational efficiency than a DSMC based method.

The recent studies have shown that while the application of the kinetic approach has a number of benefits, which include but are not limited to capturing non-equilibrium features of the condensation process and correct prediction of many condensation phenomena and rates (see, for example, Refs. [7, 13]), it does suffer from large uncertainties in key parameters used, such as heat capacities, binding energies, energy redistribution mechanism, and cluster inelastic

collision number. Some physical parameter uncertainties have been clarified in the previous paper [13], although the energy redistribution mechanisms in cluster formation and monomer-cluster collisions are still largely unknown.

The main objective of this work is the study of the energy transfer between translational and internal modes in collisions between argon dimers and monomers, and evaluation of the applicability of the phenomenological Larsen-Borgnakke model to simulate this transfer. The molecular dynamics method is used to compute realistic energy transfer cross sections and energy redistribution after collisions.

IMPACT OF THE INTERNAL ENERGY TRANSFER RATE

It has been previously noted [7] that the transfer of energy between translational and internal modes in collisions between dimers and monomers has a strong impact on the dimer equilibrium constant. The reason for this is that dimer-monomer collisions are the principal factor that changes dimer internal energy. The dimer internal energy, in turn, directly affects the dimer dissociation rate and, therefore, the equilibrium constant. The dimer dissociation is an endothermic process, and may be considered as a result of unimolecular dissociation of Ar_2 clusters that have internal energy larger than the binding energy. It is obvious that the lower the dimer binding energy, the larger the impact of the dimer internal energy relaxation rate. In Ref. [7] the cluster internal energy relaxation number Z was introduced, similar to the rotational and vibrational relaxation numbers of gas molecules, where Z is the average number of collisions allowed before one inelastic collision. It was found that Z has a much stronger influence on the argon cluster nucleation process than on water cluster nucleation, which is related to the Ar_2 binding energy E_b of 1.98×10^{-21} J, as compared to water dimer E_b of 2.455×10^{-20} J. Due to the larger E_b, a water dimer is much less likely to dissociate (for $T \approx 300$ K as in the cases of interest here), so the net nucleation rate is much less sensitive to internal energy transfer.
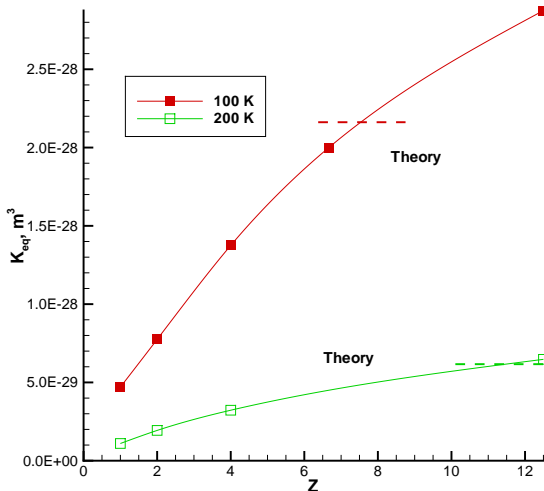
1: **FIGURE 1.** Impact of cluster internal energy relaxation rate on equilibrium constant and comparison with theoretical predictions [14].
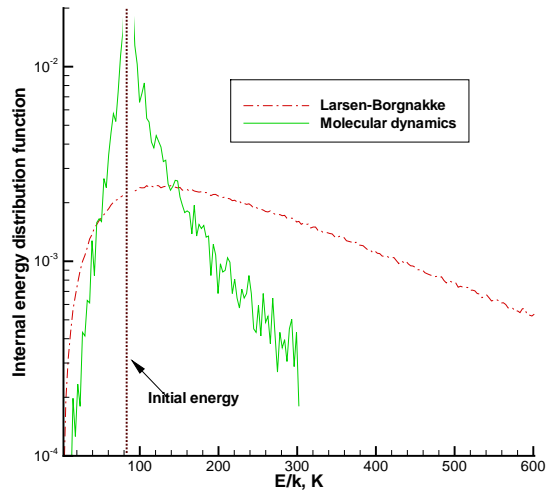
2: **FIGURE 2.** After-collision internal energy redistribution in inelastic LB and MD collisions. Initial internal energy levels are v=2, J=20 ($E_{int}/k = 83.4$ K), $T^\star = 2$.

For stable argon dimers in the temperature regime of interest, it typically takes only few collisions to exceed E_b. Although dimers with after-collision internal energy larger than the binding energy do not dissociate immediately after collision, their lifetime (the RRK model [15] may be used to estimate the cluster lifetime) is typically shorter than the mean collision time. This makes the dissociation of dimers with $E_{int} > E_b$ likely. The impact of Z on the argon dimer equilibrium constant K_{eq} is illustrated in Fig. 1, where the model [7] is used to calculate K_{eq} in a thermal bath of pure argon with a density of 1.326 kg/m^3. Note that the dependence on gas density in this case is negligible, since the mean collision time is much larger than the average cluster lifetime. The value of Z was varied from 1 to 12.5 for two gas temperatures. As expected, the increase of Z results in significant increase of the resulting equilibrium constant. The dependence on Z is almost linear at small Z, but becomes weaker as Z increases. This is because the monomer-dimer sticking becomes dominant for $Z \gg 1$ (the sticking coefficient was 0.06 for this case). As seen from the figure, the

selection of an optimum value of Z that provides the best agreement with the theoretical results of Ref. [14] depends on thermal bath temperature. It is about 7 for 100 K and 12 for 200 K. The temperature dependence used in Ref. [13] is summarized in Table 1.

NUMERICAL APPROACH

A general chemical dynamics program VENUS [16] has been used in molecular dynamics simulations. The Morse pairwise potential was applied to describe the inter- and intra-cluster interactions of argon atoms. Note that although this is a less accurate interaction potential than a more sophisticated HFDID1 potential [17], it has very similar binding energy, and is expected to provide qualitatively similar results. The Morse potential is represented in its standard form

$$V(r) = D(\exp(-2\alpha(r - r_e)) - 2\exp(-\alpha(r - r_e))$$

with the following parameters taken from [18]: α=0.908597, D=99 cm^{-1}, r_e=3.757 Å. Trajectories started at a separation of 13Åbetween dimer center of mass and impinging atoms. The convergence of cross section for various impact parameters and number of trajectories was studied, and for typical runs a maximum impact parameter of 10Å was used, and 20000 trajectories were run. Trajectories were terminated when the distance between the dimer center of mass and impinging atom was 13Å. The collision velocities were sampled from a Maxwellian distribution characteristic of the temperature (T) specified.

The gas thermal bath cases were simulated with the DSMC code SMILE [19] where the first-principles model [7, 13] was incorporated. In the expression [20] to estimate the collision complex lifetime, Lennard-Jones parameters were used: $\varepsilon = 1.98 \times 10^{-21}$ J and $\sigma = 3.405$ Å. The monomer vibration frequency in argon clusters was found to be 2.6×10^{11} s^{-1}. Finally, a collision complex stabilization probability during three-body collisions of 0.2 was used at all T.

AFTER-COLLISION ENERGY REDISTRIBUTION

The previous model [7] assumed the Larsen-Borgnakke type energy redistribution after inelastic argon monomer-dimer collisions, with the inelastic collision number Z fitted to match the dimer formation equilibrium constant as a function of temperature (see Table 1). While this approach appears reasonable for preserving correct dimer mole fractions at equilibrium, it does not guarantee proper energy distributions, trimer and larger cluster formation rates, or even dimer formation rates in non-equilibrium plume flows. In order to analyze the reliability and applicability of this approach, more accurate analysis is necessary, such as that of trajectory calculations with a realistic interaction potential.

The profiles of the after-collision internal (the sum of rotational and vibrational) energy of argon dimers is presented in Fig. 2 for two different approaches, the molecular dynamics trajectory calculations and the Larsen-Borgnakke inelastic collision algorithm. The calculations were conducted for the initial vibrational level $v = 2$ and rotational level $J = 20$ and the Maxwellian distribution of relative collision velocities at a temperature of $T^\star = 2$. Here $T^\star$ is the temperature normalized by the reduced argon dimer bond energy of $E_b/k = 143.2$ K. Only dimer-monomer collisions that resulted in net dimer internal energy change were considered for this plot. It is seen that there is a qualitative difference in the after-collision distributions, as the MD collisions tend to cause only a small change in the dimer internal energy, whereas the LB approach results in a Boltzmann distribution at a local temperature of about 185 K.

Stable argon dimers are those with internal energy smaller than E_b, that is the particles that fall to the left of $E_b/k = 143.2$ K in the after-collision energy distribution profile. The dimers with internal energy in excess of E_b are unstable or metastable and may dissociate before the next binary collision. Note that the time to dissociation may be estimated, for example, using the RRK model and is generally on the order of the inverse dimer vibration frequency of 2.6×10^{11} s^{-1}. For a 1 atm and 300 K argon gas, where the dimer mean collision time is on the order of 10^{-10} s, most unstable dimers will dissociate before the next collision. In order to create a realistic number of unstable dimers after a single collision, a parameter Z needs to be used in the LB procedure, so only a fraction $1/Z$ of collisions lead

to the internal energy transfer. The use of Z will result in a proportional decrease of the dashed line in Fig. 2, but will not change the equilibrium shape of that curve, characterized by relatively large population of high-energy tail.

We note that, in the realm of rotational energy transfer, the difference between a realistic state-to-state cross section model and a simplified LB model on the rotational distribution function after a single collision has been examined previously [21]. A completely analogous result was obtained in that study: the LB model changes the shape far too much in a single inelastic collision, but adjusts by only allowing inelastic collisions with probability $1/Z$. The LB model is expected to give reasonable results in two regimes: when only the average internal energy is important rather than the energy distribution function, or when the distribution function is important after $\sim Z$ collisions. In the case of condensation nuclei formed under strongly nonequilibrium conditions, it is possible that the LB model may not give reasonable results. Other energy transfer models that are still highly simplified but retain a slightly more realistic behavior may be needed such as that in Ref. [22].

DIMER BREAKUP CROSS SECTIONS IN DIMER-MONOMER COLLISIONS

The argon dimers are characterized by a fairly low binding energy, which results in a high probability of formation of unstable dimers after dimer-monomer collisions, followed by dimer breakup. Therefore, it is important to analyze the stable-to-unstable (or dimer breakup) collision cross sections at different gas temperatures. From these collision cross sections, obtained with the MD approach, the inelastic collision number for dimer-monomer collisions may be evaluated for a given intermolecular potential that specifies the total collision cross section (such as the VHS model in DSMC). Consider first the impact of the vibrational level v and the rotational level J of a colliding argon dimer on the cross section of a process that transforms a stable dimer with the internal energy $E_{int} < E_b$ to an unstable dimer with $E_{int} > E_b$. The MD results obtained for different v and J are shown in Fig. 3. As expected, the cross section generally increases with rotational and vibrational level, which reflects the increase of the dimer breakup probability with the available internal energy of the colliding dimer. Note that the stable-to-unstable dimer cross section is more sensitive to the change in vibrational level, Fig. 3 (left), where the energy quantum is larger; the cross section increase is relatively insignificant for small rotational numbers, Fig. 3 (right), due to the J^2 dependence of the internal energy.
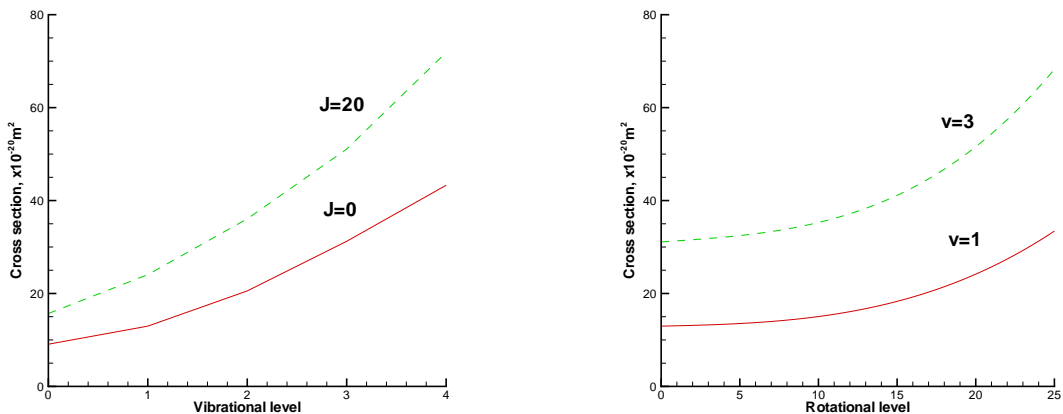

FIGURE 3. Stable-to-unstable dimer cross section as a function of changing vibrational (left) or rotational (right) level. $T^\star = 0.5$.

The increase of the cross section with the rotational quantum number is more pronounced at lower temperatures, as illustrated in Fig. 4 (left). This is related to the fact that at $T^\star = 2$, the average relative translational energy is noticeably larger than E_b, and thus the pre-collision rotational energy is relatively less important than for $T^\star = 0.5$. The average internal energy of stable dimers (over the range of $T^\star$ in the figure) changes between $E_{int}/k = 78$ K and $E_{int}/k = 92$ K, and the dimer breakup cross section for a typical internal energy of 84 K ($v = 2$ and $J = 20$) is shown in Fig. 4 (right). It is interesting to note that the breakup cross section practically does not change after $T^\star \approx 1$. This indicates that dimer breakup probability, which is the ratio of the breakup cross section to the total collision cross section σ_{tot}, will only be a function of σ_{tot} at $T \approx 140K$. For a lower internal energy ($v = 2$ and $J = 4$), the temperature dependence is more noticeable, but still relatively weak.
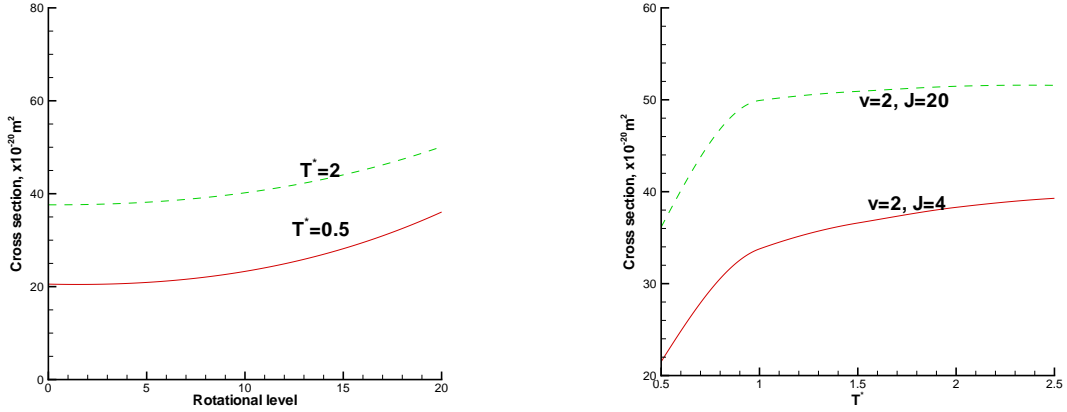
FIGURE 4. Stable-to-unstable dimer cross section for $v = 2$ and two different translational temperatures (left) and for two different internal states and varying translational temperature (right).

DIMER BREAKUP AND INELASTIC PROBABILITIES

The most important outcome of collisions between stable dimers (which form the nuclei from which larger clusters can be grown) and monomers is the production of unstable dimers with internal energy larger than the binding energy, since this is the main mechanism of nucleus destruction. Its impact on dimer population will in turn influence the population of larger clusters, that are created through sticking and coalescence of dimers. For the condensing gas model to be reliable, it is important to implement correct rates of breakup and therefore correct cross sections for inelastic collisions leading to dissociation.

For a kinetic condensation model that is based on VHS total collision cross sections and the LB energy redistribution algorithm, the value of the inelastic collision number Z can be related to the dissociation cross section as follows: $Z^{-1} = \phi = \sigma_{MD}/\sigma_{LB}$, where ϕ is the probability of the collisional energy transfer that results in the formation of an unstable dimer, σ_{MD} is the dimer dissociation cross section obtained from molecular dynamics simulations (or experiment, or other method considered reliable), and σ_{LB} is the dimer breakup cross section in a single VHS collision at the given collision energy that undergoes LB energy transfer between all translational and internal energy modes. The results of calculation of ϕ for different rotational and vibrational levels and translational temperatures are summarized in Table 2.

Two conclusions may be drawn from this table. First, the MD calculations indicate that for a given internal energy, the dimer with a higher vibrational energy will break up with higher probability (vibrational favoring). Second, and most importantly, for given vibrational and rotational levels, Z^{-1} significantly decreases when the translational temperature increases. For example, for the reduced internal energy of 83.89 K, $\phi = 1/Z$ decreases by a factor of 2, from 0.605 to 0.306, when the gas temperature increases from $T^\star = 0.5$ to 2. A similar temperature dependence is observed when Z is calculated in a conventional manner based on energy relaxation to equilibrium value (as in Fig. 1). Note that for larger dimer internal energies, the values of ϕ approach unity. The MD cross sections are noticeably lower than the VHS total collision cross section for dimer-monomer interactions of 220Å. While the values of ϕ calculated as $\phi = \sigma_{MD}/\sigma_{LB}$ may be directly used in modeling condensing flows with a kinetic approach such as that of Ref. [7], the use of the LB technique for energy transfer in dimer-monomer collisions results in drastically different from MD energy redistribution, which may lead to inaccurate results. Therefore, it is better to evaluate ϕ from comparison with equilibrium dimer formation rates, and select the values that provide a good agreement with available theoretical results. It was found from comparison with theoretical analysis [14] that $\phi = 0.2$ for equilibrium gas at $T^\star = 0.7$, 0.11 for $T^\star = 1.4$, and 0.08 for $T^\star = 2.1$. This presents a temperature dependence similar to that obtained with $\phi = \sigma_{MD}/\sigma_{LB}$, although with a smaller magnitude of the inelastic collision probability. The above values differ somewhat from those in Table 1 because of the difference in the physical parameters described in the Numerical Approach section.

TABLE 2. Droplet breakup cross sections for different internal energies.

v	J	$\frac{E_{int}}{k}$, K	σ_{MD}, Å^2	σ_{LB}, Å^2	ϕ
			$T^\star = 0.5$		
0	0	11.71	9.08	29.85	0.30
0	10	20.87	10.71	32.75	0.33
0	20	46.11	15.68	42.06	0.37
0	30	85.60	32.83	60.63	0.54
2	0	53.53	20.55	45.16	0.46
2	10	61.64	23.31	48.77	0.48
2	20	83.89	36.06	59.71	0.60
2	30	115.82	70.07	78.03	0.90
4	0	87.32	43.29	61.55	0.70
4	10	94.32	48.69	65.44	0.74
4	20	113.25	71.88	76.46	0.94
			$T^\star = 2$		
2	0	53.53	37.64	157.05	0.24
2	10	61.64	40.36	158.93	0.25
2	20	83.89	50.13	164.00	0.31
2	30	115.82	81.78	170.90	0.48

CONCLUSIONS

Molecular dynamics calculations of energy transfer in argon dimer-monomer collisions have been performed, with emphasis on collisions that result in formation of unstable dimers with internal energy larger than the binding energy. Comparison with the energy transfer algorithm based on VHS and Larsen-Borgnakke models for total and inelastic cross sections indicates that the inelastic collision number decreases strongly with temperature. The large differences between the after-collision internal energy distributions in MD and LB models, as well as the presence of vibrational favoring in MD, emphasize the highly simplified phenomenological nature of the LB model and indicate that it may not be adequate for simulating the physics and kinetics of nucleation, but further study is needed to understand the shortcomings in detail. In addition, the situation for energy transfer to higher clusters ($N > 2$) of argon or clusters of molecular species is completely unknown and requires attention.

REFERENCES

1. S.F Simmons, *Rocket Exhaust Plume Phenomenology*, The Aerospace Corporation Aerospace Press Series, AIAA (2000).
2. L. Prandtl, *Atti del Convegno Volta*, 1st edn., vol. XIV. Roma: Reale Academia D'Italia (1936).
3. X. Luoǎ, G. Lamanna, A. P. C. Holten, M. E. H. van Dongen, J. Fluid Mech., **572**, 339-366 (2007).
4. J. Zhong, D. Levin, AIAA Journal, **45** (4), 902-911 (2007).
5. Z. Li, J. Zhong, D.A. Levin, B.J. Garrison, AIAA Journal, **47 (5)**, 1241-1251 (2009).
6. B. Briehl, H. Urbassek, J. Vac. Sci. Tech. A, **17** (1), 256 (1999).
7. R. Jansen, S. Gimelshein, M. Zeifman, I. Wysong, AIAA Paper 2009-3745 (2009).
8. R. Jansen, I. Wysong, S. Gimelshein, M. Zeifman, and U. Buck, J. Chem. Phys. **132**, 244105 (2010).
9. R.D. Levine, *Molecular reaction dynamics*, Cambridge University Press (2005).
10. S.F. Gimelshein, M.S. Ivanov, in Rarefied Gas Dynamics XVII, Progress in Astronautics and Aeronautics, **159**,218-233 (2004).
11. C. Borgnakke, P.S. Larsen, J. Comp. Phys. **18**, 405 (1975).
12. R. Jansen, S. Gimelshein, N. Gimelshein, I. Wysong, AIAA Paper 2010-5011 (2010).
13. A. Borner, Z. Li, D. Levin, R. Jansen, S. Gimelshein, I. Wysong, AIAA Paper 2010-985 (2010).
14. P.S. Dardi, J.S. Dahler, J. Chem. Phys, **93** (5), 3562-3572 (1990).
15. R.D. Levine, Molecular reaction dynamics, Cambridge University Press, 2005.
16. W. L. Hase, et al., Quantum Chem. Program Exch., **16**, 671 (1996).
17. R. A. Aziz, J. Chem. Phys., **99**, 4518 (1993).
18. P. N. Roy, J. Chem. Phys., **119**, 5437 (2003).
19. M.S. Ivanov, G.N. Markelov, S.F. Gimelshein, Computers and Mathematics with Applications, **35** (1-2), 113-126 (1998).
20. D.L. Bunker, J. Chem. Physics, **32**(4), 1001-1005 (1959).
21. I.J. Wysong and D.C. Wadsworth, Phys. Fluids **10**, 2983 (1998).
22. D.I Pullin, Phys. Fluids **21**, 210 (1978).